The Astrophysical Journal, 795:115 (8pp), 2014 November 10 doi:10.1088/0004-637X/795/2/115


# OPTICAL COUNTERPARTS OF TWO *FERMI* MILLISECOND PULSARS: PSR J1301+0833 AND PSR J1628−3205

Miao Li[1], Jules P. Halpern[1], and John R. Thorstensen[2]
[1] Department of Astronomy, Columbia University, 550 West 120th Street, New York, NY 10027, USA; miao@astro.columbia.edu
[2] Department of Physics and Astronomy, Dartmouth College, Hanover, NH 03755, USA
*Received 2014 July 30; accepted 2014 September 11; published 2014 October 21*

## ABSTRACT

Using the 1.3 m and 2.4 m Telescopes of the MDM Observatory, we identified the close companions of two eclipsing millisecond radio pulsars that were discovered by the Green Bank Telescope in searches of *Fermi Gamma-ray Space Telescope* sources, and measured their light curves. PSR J1301+0833 is a black widow pulsar in a 6.5 hr orbit whose companion star is strongly heated on the side facing the pulsar. It varies from $R = 21.8$ to $R > 24$ around the orbit. PSR J1628−3205 is a "redback," a nearly Roche-lobe-filling system in a 5.0 hr orbit whose optical modulation in the range $19.0 < R < 19.4$ is dominated by strong ellipsoidal variations, indicating a large orbital inclination angle. PSR J1628−3205 also shows evidence for a long-term variation of about 0.2 mag, and an asymmetric temperature distribution possibly due to either off-center heating by the pulsar wind, or large starspots. Modeling of its light curve restricts the inclination angle to $i > 55^\circ$, the mass of the companion to $0.16 < M_c < 0.30\,M_\odot$, and the effective temperature to $3560 < T_{\rm eff} < 4670$ K. As is the case for several redbacks, the companion of PSR J1628−3205 is less dense and hotter than a main-sequence star of the same mass.

*Key words:* gamma rays: stars – pulsars: individual (PSR J1301+0833, PSR J1628−3205)

## 1. INTRODUCTION

Millisecond pulsars (MSPs) are neutron stars (NSs) that are spinning faster than any young pulsar. Shortly after their discovery, the "recycling" model was proposed by Alpar et al. (1982) and Radhakrishnan & Srinivasan (1982) to explain how MSPs acquire such high rotation velocity: they were previously spun up by accretion through Roche-lobe overflow of their companions in low-mass X-ray binaries (LMXBs) as the orbit shrinks due to magnetic braking and/or gravitational radiation. This scenario is consistent with the preponderance of MSPs in binary systems, and it also explains the fact that they have much weaker magnetic fields than ordinary pulsars, since accretion can dissipate and bury magnetic field (Romani 1990; Geppert & Urpin 1994).

An interesting subclass of MSPs are the eclipsing radio MSPs, the so-called "black widows" and "redbacks." Approximately 53 such systems are known[3] from large-scale radio surveys, deep searches of globular clusters, and most recently, radio follow-ups of unidentified *Fermi* $\gamma$-ray sources (e.g., Hessels et al. 2011; Ransom et al. 2011; Ray et al. 2012). Black widows and redbacks are compact binaries with short orbital periods ($\lesssim$1 day) and small companion masses, $\approx$0.01–0.05 $M_\odot$ for black widows, and $\approx$0.1–1 $M_\odot$ for redbacks. Radio eclipses occur when the pulsar is at superior conjunction. The eclipsing plasma is usually more extended than the Roche lobe of the companion, which motivated the theory that the companion is being ablated by the high-energy particles and/or photons from the pulsar (Phinney et al. 1988). Indeed, optical and X-ray fluxes show orbital modulation indicating that the side of the companion facing the pulsar is being heated (e.g., Romani & Shaw 2011; Kong et al. 2012; Breton et al. 2013; Gentile et al. 2014; Bogdanov et al. 2011, 2014a, 2014b).

It is unclear how black widow and redback binaries arrived at their current state, given the complexity of mass transfer and ablation. We do not even know if redbacks evolve into black widows, or if they have completely different histories. Neither fall on the normal binary evolution sequences; on the diagrams of orbital period versus companion mass and luminosity versus temperature (e.g., Figure 2 of Podsiadlowski et al. 2002), a fair fraction of redbacks appear in the gap between the evolutionary tracks of long- and short-period systems, whereas black widows occupy a completely different region. Mass loss due to irradiation may have played a role (Chen et al. 2013; Benvenuto et al. 2014). Ablation has also been suggested to explain the existence of isolated MSPs outside of globular clusters (e.g., Kluzniak et al. 1988), but it may be difficult to heat the photosphere enough to achieve the required mass flux to completely evaporate the companion (Eichler & Levinson 1988). More multi-wavelength observations and physical understanding of pulsar wind interaction with stellar material are needed to resolve these issues.

Recently, transitions from accretion mode to radio MSPs have been found in several redback systems (PSR J1023+0038, PSR J1824−2452I, and XSS J12270−4859) that decline in X-ray luminosity and exhibit millisecond radio pulsations (Archibald et al. 2009; Papitto et al. 2013; Roy et al. 2014). Optical spectra also show that the blue continuum and double-peaked emission lines from accretion disks have been replaced by pure stellar absorption (e.g., Thorstensen & Armstrong 2005; Wang et al. 2009; Bassa et al. 2014). The opposite transitions have also been observed in PSR J1824−2452I (Papitto et al. 2013) and PSR J1023+0038 (Stappers et al. 2013; Halpern et al. 2013). X-ray luminosities in the accretion state vary by orders of magnitude, from $>10^{36}$ erg s$^{-1}$, which is similar to a typical LMXB, to a mild increase from the MSP mode (Linares 2014). The fast transitions and variations of luminosity reveal that the binary interaction is complex, and the mass transfer rate is not always high enough for the accretion disk to reach the NS and spin it up. With multi-wavelength monitoring, we expect to see more transitions between accretion- and rotation-powered states.

Black widows and redbacks are ideal systems to measure NS mass, since the orbital radial velocity of pulsar and companion

[3] http://apatruno.wordpress.com/about/millisecond-pulsar-catalogue/

**Table 1**
Log of Observations

| Object | Telescope | Date (UT) | Time (UT) | Orbital Phase ($\phi$)[a] |
|---|---|---|---|---|
| PSR J1301+0833 | 1.3 m | 2013 Apr 4 | 04:29–08:50 | 0.76–0.13 |
| " | 2.4 m | 2014 May 26 | 03:45–05:40 | 0.73–0.02 |
| " | 2.4 m | 2014 May 27 | 03:32–05:54 | 0.43–0.72 |
| " | 2.4 m | 2014 May 28 | 04:48–05:20 | 0.23–0.31 |
| PSR J1628−3205 | 1.3 m | 2013 Apr 7 | 09:30–12:18 | 0.57–0.13 |
| " | 1.3 m | 2013 Jul 7 | 05:35–07:02 | 0.99–0.25 |
| " | 2.4 m | 2014 May 26 | 05:58–09:36 | 0.88–0.60 |
| " | 2.4 m | 2014 May 27 | 06:04–09:37 | 0.70–0.40 |
| " | 2.4 m | 2014 May 28 | 05:34–09:28 | 0.41–0.18 |

**Note.** [a] Phase zero corresponds to the ascending node of the pulsar.

can be measured separately through radio and optical Doppler shifts, respectively, and light-curve modeling can constrain the inclination angle of the orbit. Of special interest is that these NSs tend to be more massive due to the previous long accretion phases. Romani et al. (2012), for example, have found the black widow PSR J1311−3430 very likely to have $M_{\rm NS} > 2.1\,M_\odot$. This probe of the upper limit of NS mass helps to constrain the equation of state for super-dense matter, enabling us to explore fundamental physics under extreme conditions that are unachievable on the Earth (Lattimer & Prakash 2007, and references therein).

Here we report optical identifications and light curves of two binary MSPs that were discovered in a radio survey of *Fermi* sources using the Green Bank Telescope (GBT; PI: S. Ransom) and subsequently timed with the GBT and the Westerbork Synthesis Radio Telescope to determine their orbital and spin-down parameters (J. Hessels et al., in preparation). PSR J1301+0833 is a 1.84 ms black widow in a 6.5 hr orbit (Ray et al. 2012), while PSR J1628−3205 is a 3.21 ms redback in a 5.0 hr orbit. We use the light curve of PSR J1628−3205, together with the pulsar orbital ephemeris, to constrain some properties of the system. The paper is organized as follows: we describe our observations and data reduction in Section 2. In Section 3 we describe the light-curve fitting model and present its results for PSR J1628−3205. We discuss our findings in Section 4, and summarize our conclusions in Section 5.

## 2. OBSERVATIONS

All of our data are from *R*-band images obtained at the MDM Observatory's 1.3 m McGraw-Hill Telescope or 2.4 m Hiltner Telescope on Kitt Peak during three observing runs in 2013 and 2014. A log of the time-series observations used in this paper is presented in Table 1. The detector was the thinned, backside-illuminated SITe CCD "Templeton." It has 1024 × 1024 pixels, with a scale of 0.″509 pixel$^{-1}$ on the 1.3 m, and 0.″275 pixel$^{-1}$ on the 2.4 m. All exposures were 300 s, and readout time was ≈30 s. The runs were timed to eventually cover all orbital phases of each pulsar. The data were reduced using standard procedures in IRAF, including bias-subtraction, flat-fielding with twilight exposures, and differential aperture photometry with respect to isolated comparison stars using *phot*. Photometric calibration of the comparison stars was done using Landolt (1992) standard stars observed immediately before or after the target pulsars. Heliocentric correction was applied to the light curves.

### 2.1. PSR J1628−3205

PSR J1628−3205 is the only one of a group of six redback systems in the Galactic field from Roberts (2013) that remains to be identified optically. Optical studies have revealed that redback companion stars are hot, with $T_{\rm eff} \approx 5000$–$6000$ K, and fill a large fraction of their Roche lobes (Breton et al. 2013; Crawford et al. 2013; Schroeder & Halpern 2014). An exception is PSR J1816+4510, which is significantly hotter, $T_{\rm eff} \approx 16{,}000$ K, and underfills its Roche lobe (Kaplan et al. 2012, 2013). Existing data suggest they are metal-rich and non-degenerate, consistent with the expectation that the outer layers have been ablated and the remnant stars are bloated by heating, but their exact nature is still not clear. The minimum mass of the companion to PSR J1628−3205 is $M_c = 0.16\,M_\odot$ if $M_{\rm NS} = 1.4\,M_\odot$.

The pulsar dispersion measure (DM) of 42.1 pc cm$^{-3}$ for PSR J1628−3205 (Ray et al. 2012) corresponds to a distance $d = 1.24$ kpc according to the Cordes & Lazio (2002) model of the Galactic distribution of free electrons. We will assume a nominal uncertainty of ±30% on the distance for the purpose of modeling in Section 3, but we will also allow for an error of a factor of ∼2, which sometimes occurs, especially at high Galactic latitude (e.g., Roberts 2011; Deller et al. 2012). The 0.1–100 GeV luminosity of the *Fermi* source 2FGL J1628.3−3206 at this distance is $\approx 2.1 \times 10^{33}$ erg s$^{-1}$ (assumed isotropic), which is 16% of its apparent spin-down luminosity, $\dot{E} = 4\pi^2 I \dot{P}/P^3 = 1.29 \times 10^{34}$ erg s$^{-1}$ from the timing parameters (S. Ransom 2014, private communication). This is a typical $\gamma$-ray efficiency for MSPs. Here we have assumed the moment of inertia $I = 1 \times 10^{45}$ g cm$^2$, which could be uncertain by a factor of two. The precise radio timing position coincides with a faint star on the digitized sky survey, with magnitudes $B2 = 21.06$, $R2 = 18.61$ in the USNO-B1.0 catalog (Monet et al. 2003). In images obtained on the 1.3 m (Figure 1) we refined its optical position to (J2000.0) R.A. = 16$^{\rm h}$28$^{\rm m}$07.$^{\rm s}$02, decl. = −32°05′48.″7 in the USNO-B1.0 reference frame.

Due to the southerly declination of PSR J1628−3205, as well as partly cloudy conditions, we were only able to observe ≈68% of the phase of its 6.0 hr orbit using the 1.3 m in 2013. Nevertheless, the coverage was complete enough to reveal that there are two flux minima and two maxima per orbit (Figure 2), a modulation consistent with ellipsoidal deformation of a nearly Roche-lobe-filling star in a highly inclined orbit. The basic manifestations of ellipsoidal variations are (1) equal maxima at quadrature phases (0.0 and 0.5) when the projected area of the tidally distorted star is largest, and (2) unequal minima at phases 0.25 and 0.75 due to the larger effects of gravity darkening and limb darkening when viewing the L1 point of the companion star at $\phi = 0.75$. Fitting of the light curve including these effects will be presented in Section 3. Evidently, heating of the companion by the pulsar wind, which should contribute most at $\phi = 0.75$, is not a major effect in this system.

In 2014 May, we obtained additional light curves of PSR J1628−3205 using the MDM 2.4 m Telescope (Figure 3). As before, all observations were obtained at high airmass, sec $z = 2.3$–$2.9$. Although it took three nights to cover all orbital phases, the substantial overlap in phase among the nights shows that the light curve is largely stable over this time interval. The higher precision of the 2.4 m data establishes three interesting properties of the light curve. First, the two maxima, at $\phi = 0.0$ and 0.5, are not quite equal, differing by ≈0.1 mag. This implies that the temperature distribution on the companion is not symmetric about the axis connecting the stars. The

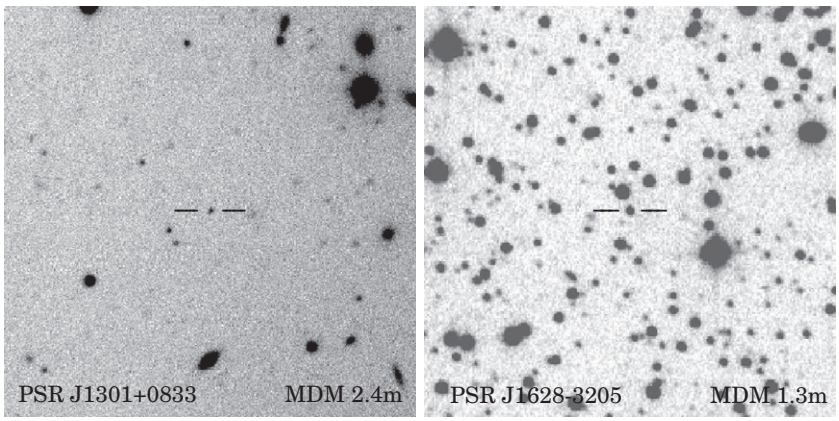


**Figure 1.** Finding charts for PSR J1301+0833 (left) and PSR J1628−3205 (right), taken from MDM *R*-band images. Positions are (J2000.0) R.A. = $13^{h}01^{m}38\overset{s}{.}26$, decl. = $+08^{\circ}33'57\overset{''}{.}5$ and R.A. = $16^{h}28^{m}07\overset{s}{.}02$, decl. = $-32^{\circ}05'48\overset{''}{.}7$, respectively. The size is $2' \times 2'$. North is up, and east is to the left.

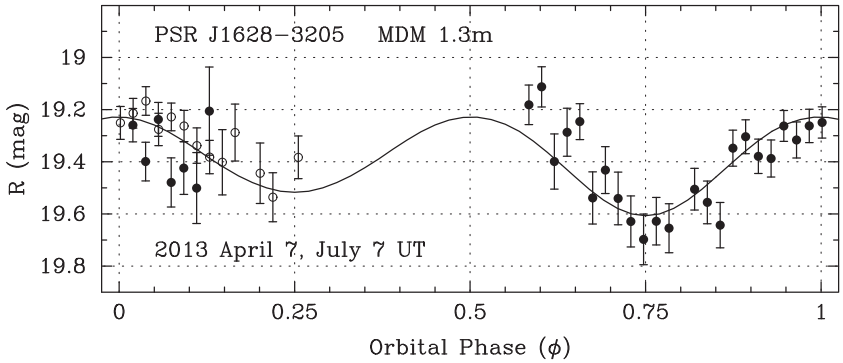


**Figure 2.** *R*-band light curve as a function of orbital phase for PSR J1628−3205. Filled circles are from 2013 April 7, and open circles from 2013 July 7, both from the MDM 1.3 m Telescope. Phase zero corresponds to the ascending node of the pulsar, so $\phi = 0.75$ is the superior conjunction of the companion star. The curve is a model of ellipsoidal modulation described in Section 3, with $d = 1.24$ kpc, $M_{\rm NS} = 1.4\,M_{\odot}$, $M_c = 0.167\,M_{\odot}$, $i = 75^{\circ}$, and $T_{\rm eff} = 4130$ K.

trailing side of the companion is brighter. Second, the deeper minimum in the light curve, which is expected to fall exactly at $\phi = 0.75$, lags by about 0.05 in phase, while the minimum at $\phi = 0.25$ is not displaced. These two effects could indicate heating from the pulsar that is not symmetric about the line between the stars, but stronger on the trailing side of the companion. Alternatively, there could be an intrinsic temperature distribution resulting from large starspots. The third interesting result is an increase in brightness from the previous year (Figure 2) by an amount that ranges from 0.1 to 0.2 mag around the orbit. This could be due to an increase in the radius or temperature of the photosphere, perhaps from enhanced heating by the pulsar. Historical detections of PSR J1628−3205 on the Digitized Sky Survey plates are broadly consistent with our CCD magnitudes, but they are too uncertain to be evaluated for additional evidence of variability.

We note that the magnitude scale in Figures 2 and 3 may have a systematic error of ∼0.05 mag due to the difficulty of photometric calibration at large airmass. Nevertheless, the three effects described in the previous paragraph, which rely only on differential photometry, have been checked with several comparison stars, and they appear to be reliable.

We were able to test for proper motion of PSR J1628−3205 by comparing its position on our CCD images with a UK Schmidt IV-N plate that was taken on 1980 July 16. The latter provides the best detection of PSR J1628−3205 of any of the digitized sky survey plates. Employing a surrounding grid of 29 stars with positions and proper motions in the USNO-B1.0 catalog as astrometric references, we calculate proper motion in right Ascension (R.A.) and declination (decl.) as $\mu_{\alpha}\cos\delta = +8 \pm 9$ mas yr$^{-1}$ and $\mu_{\delta} = -16 \pm 9$ mas yr$^{-1}$, respectively. The errors are dominated by the accuracy of centroiding the object on the digitized plate image, which we take to be $0\overset{''}{.}3$ in each coordinate. Although only a marginal detection of motion, this corresponds to a tangential velocity of ∼100 km s$^{-1}$ at $d = 1.2$ kpc, which is relevant to the estimation of the true spin-down rate of the pulsar as discussed in Section 4.

An observation of PSR J1628−3205 with the *Chandra X-ray Observatory* ACIS-S3 CCD detected ≈176 photons, ranging in energy from 0.4 to 7 keV, from a point source at (J2000.0) R.A. = $16^{h}28^{m}07\overset{s}{.}00$, decl. = $-32^{\circ}05'48\overset{''}{.}9$, consistent with our optical position and the radio timing position. The 20 ks exposure on 2012 May 2 (ObsID 13725) spanned 1.25 orbits of the pulsar. In Figure 4 we show the arrival times and energies of those photons as a function of orbital phase. There is no apparent orbital modulation of count rate or photon energy, indicating that the X-rays are probably coming from the pulsar, and not an intra-binary shock near the companion star (where they could be partly occulted by the companion). If so, the hard X-rays (above 2 keV) indicate a preponderance of non-thermal magnetospheric emission over thermal emission from heated polar caps, which is unusual for MSPs of the spin-down power of PSR J1628−3205.

### 2.2. PSR J1301+0833

The minimum mass of the companion to PSR J1301+0833 is $M_c = 0.024\,M_{\odot}$ if $M_{\rm NS} = 1.4\,M_{\odot}$, making this a likely black widow system. The DM of 13.2 pc cm$^{-3}$ for PSR J1301+0833

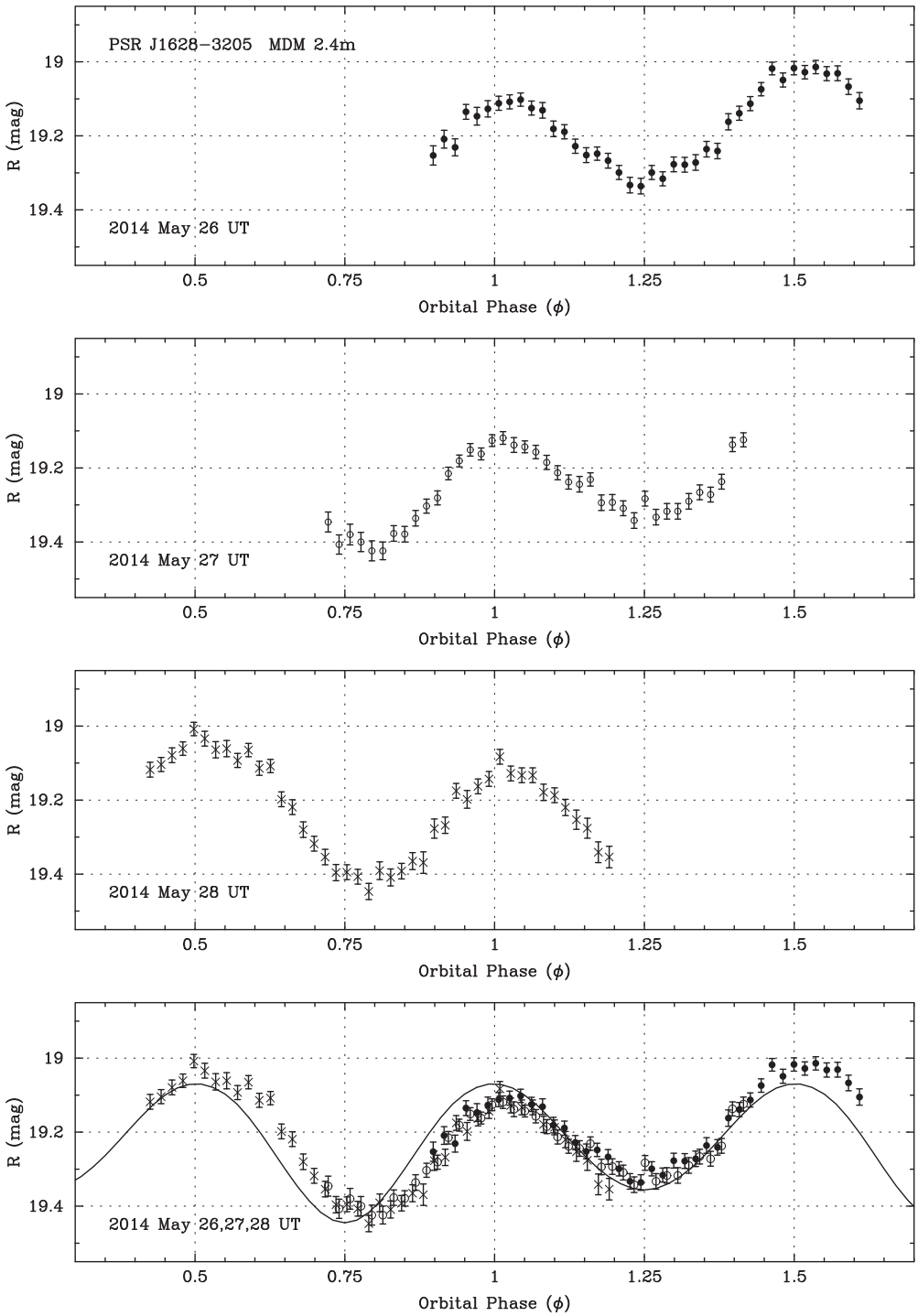


**Figure 3.** *R*-band light curves as a function of orbital phase for PSR J1628−3205, obtained on three consecutive nights in 2014 May, on the MDM 2.4 m. The bottom panel shows the points from the three nights superposed, retaining their different symbols from the individual nights. The curve is the representative ellipsoidal model described in Section 3, with $d = 1.24$ kpc, $M_{\rm NS} = 1.4\,M_\odot$, $M_c = 0.167\,M_\odot$, $i = 75°$, and $T_{\rm eff} = 4230$ K.

(Ray et al. 2012), corresponds to $d \approx 0.67$ kpc. The 0.1–100 GeV luminosity o f the *Fermi* source 2FGL J1301.5+0835 at this distance is $\approx 4.5 \times 10^{32}$ erg s$^{-1}$ (assumed isotropic), which is 0.9% of its apparent spin-down luminosity, $\dot{E} \approx 5 \times 10^{34}$ erg s$^{-1}$ from the timing parameters (F. Camilo 2014, private communication), corrected for proper motion. In images obtained at the 2.4 m we found a variable star at the precise radio timing position. It was also detected by the 1.3 m, although too faint there to be studied in detail. Figure 1 shows a finding chart for PSR J1301+0833 from the 2.4 m. Its position in the USNO-B1.0 reference frame is (J2000.0) R.A. = $13^{\rm h}01^{\rm m}38\overset{\rm s}{.}26$, decl. = $+08°33'57\overset{''}{.}5$.

The *R*-band light curve of PSR J1301+0833 is shown in Figure 5. The most useful data come from three consecutive nights in 2014 May, the same as were used to study PSR J1628−3205. Sharing the time between these targets, we were only able to cover the complete 6.5 hr orbit of PSR J1301+0833 by scheduling it in parts over three nights. The maximum

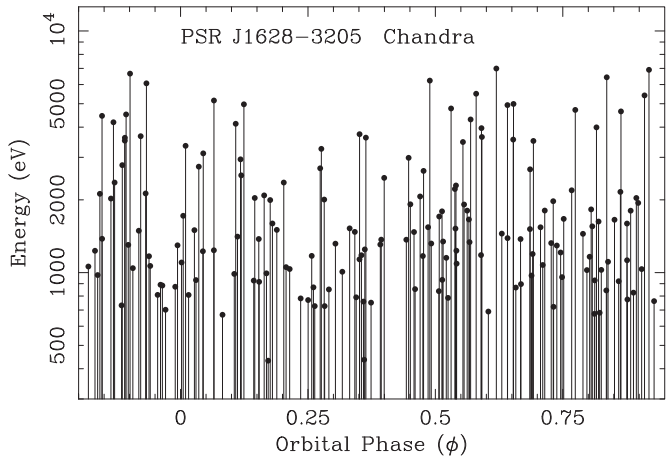


**Figure 4.** Energies and arrival times in orbital phase of 176 photons detected from PSR J1628−3205 by *Chandra* on 2012 May 2 (ObsID 13725). Each point is one photon.

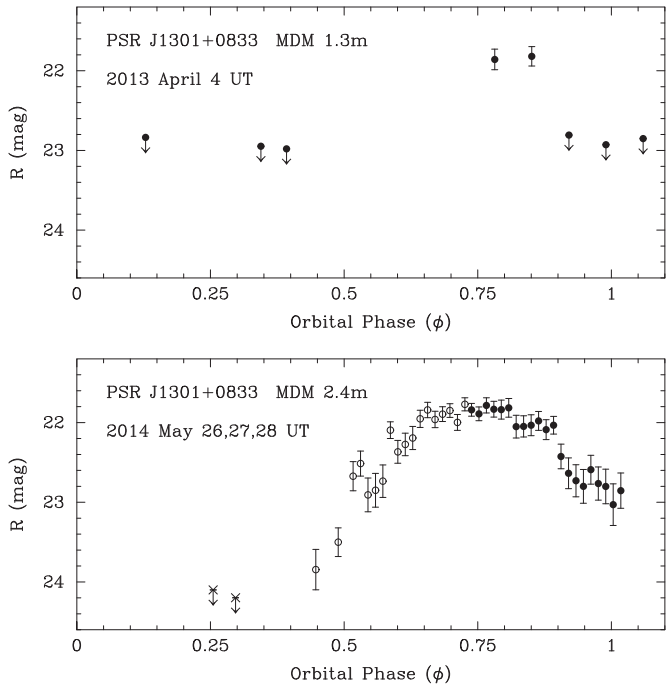


**Figure 5.** *R*-band light curve as a function of orbital phase for PSR J1301+0833, showing a heating effect peaking at phase 0.75, the superior conjunction of the companion star. Top: detections and upper limits from the MDM 1.3 m Telescope are from the sums of between three and five consecutive 300 s exposures. Bottom: data obtained on three consecutive nights in 2014 May on the MDM 2.4 m. The symbols correspond to the same dates as in Figure 3. The four lowest points are from the sums of three consecutive 300 s exposures; the remainder are individual exposures.

brightness of $R = 21.8$ occurs at phase 0.75, which is expected for maximal heating of the companion by the pulsar wind. There is a hint of flaring behavior on the rising side of the light curve, from $0.50 < \phi < 0.58$, but additional data with higher time resolution would be needed to confirm this. This star is also detected as SDSS J130138.25+083357.6 with $r = 21.86 \pm 0.12$, $i = 21.46 \pm 0.13$. Evidently the Sloan Digital Sky Survey (SDSS) caught the star near maximum light.

The night of May 28 was partly cloudy during the observations of this target, resulting in no coverage of phases 0.05–0.2 and 0.35–0.4. However, these phases are close to inferior conjunction of the companion, where it is already obvious from the upper limits that we did obtain that the intrinsic magnitude of the star is fainter than $R = 24$. These upper limits were obtained from the sums of three consecutive 300 s exposures, as were the two faintest detections at $\phi = 0.43$–0.5; the remainder of the points in Figure 5 are from individual exposures.

## 3. LIGHT-CURVE MODELING

Although the PSR J1628−3205 system is evidently not accreting, it is apparent from its large ellipsoidal variations that the secondary star nearly fills its Roche lobe. Therefore, we modeled the light curve using the code of Thorstensen & Armstrong (2005), which was designed for the redback PSR J1023+0038. It accounts for effects of gravity darkening and limb darkening, in addition to treating the pulsar as a point source of radiation that becomes thermalized in the photosphere of the companion and is re-radiated locally at the higher effective temperature needed to carry the added luminosity. The surface brightness at a given effective temperature is estimated from stellar atmosphere models.

We modified the code to make predictions for the Cousins *R* band, and removed the parts of the code that predict and fit the color modulation, since we have only one passband. The program predicts the brightness of a Roche-lobe-filling star using an approximation to the surface brightness versus $T_{\rm eff}$ relation. For the present use, in addition to adopting values appropriate to the *R* band, we extended the temperature range down to 2400 K using M-dwarf data tabulated by Casagrande et al. (2008). The limb- and gravity-darkening coefficients were not changed from their standard values in Thorstensen & Armstrong (2005).

First, we estimate the correction for interstellar extinction. At the DM distance $d = 1.24$ kpc and Galactic latitude of 11.°5, PSR J1628−3205 has a *z*-height of 250 pc, possibly placing it above most of the Galactic dust layer. The corresponding free electron column of $N_{\rm e} = 1.3 \times 10^{20}$ cm$^{-2}$, assuming a typical ionized fraction of 0.1 (He et al. 2013), is accompanied by a neutral column of $N_{\rm H} = 1.3 \times 10^{21}$ cm$^{-2}$, with an associated visual extinction of $A_V \approx 0.72$ mag according to the conversion $N_{\rm H}/A_V = 1.8 \times 10^{21}$ cm$^{-2}$ mag$^{-1}$ of Predehl & Schmitt (1995). Alternatively, the total line-of-sight dust extinction in this direction, $A_V \approx 1.07$ (Schlafly & Finkbeiner 2011), sets an upper limit to the extinction of PSR J1628−3205. Scaling to the *R* band via $A_R/A_V = 0.79$, the corresponding estimate and upper limit are $A_R \approx 0.57$ and $A_R \approx 0.85$, respectively. We adopt here $A_R = 0.75$ mag for our calculations.

The higher-quality data from the 2.4 m demonstrates that, while the light curve is dominated by ellipsoidal modulation, ellipsoidal variations alone cannot fit accurately. This is because of the unequal maxima, and the fact that the lower minimum occurs later than the expected phase of 0.75 (see Figure 3 and Section 2.1). Large magnetic spots on the secondary could plausibly explain the distortions; we did not attempt to model this. In any case, the mismatch between the data and model light curves is mostly systematic. Because of this, a formal best-fit analysis would necessarily be misleading, so we used the models only to establish broad limits on the system parameters, as follows.

*Heating effects.* If the inward face of the secondary were heated significantly by the pulsar, the minimum near phase 0.75 would be boosted, but we see no indication of that. For modeling purposes, we leave the heating luminosity from the pulsar set to zero.

*Mass range.* We assume that $M_{\rm NS}$ is between 1.4 and 2.6 $M_\odot$; the range extends to the high side because pulsars in

these systems are thought to have accreted significant mass during their spin-up. Pulsar timing gives an extremely accurate $a_{\rm NS}\sin i$, corresponding to $v_{\rm NS}\sin i = 42.972$ km s$^{-1}$, so that for any assumed $M_{\rm NS}$ and inclination $i$, the companion-star mass $M_c$ is fixed. The minimum possible companion mass for our assumed range of NS mass is $M_c = 0.161\,M_\odot$, corresponding to $M_{\rm NS} = 1.4\,M_\odot$ and $i = 90^\circ$.

*Inclination.* The amplitude of the modulation depends primarily on $i$; it also increases slightly at lower assumed $T_{\rm eff}$. After examining sample light curves, we concluded that the amplitudes predicted by models with inclination less than 55° were simply too low to match the data, so we adopt $i > 55^\circ$ as a firm limit. We cannot rule out inclinations as high as 90°. Note that adding a constant source of light, or assuming that the secondary underfills its Roche lobe, would tend to make the modulation smaller, and hence increase the lower limit on $i$.

*Effective temperature.* This is the "base" temperature, the effective surface temperature in the absence of gravity darkening. Without colors or spectra, we cannot find the secondary star's $T_{\rm eff}$ directly, but we can estimate it as follows. The large ellipsoidal modulation implies that the secondary must come close to filling its Roche lobe. Assuming a NS mass and orbital inclination, we can then compute the secondary's mass and radius. Assuming a value of $T_{\rm eff}$ then fixes the surface brightness, and hence the secondary's absolute magnitude; matching to the observed (extinction-corrected) flux then gives a distance. We can constrain $T_{\rm eff}$ by requiring the derived distance to lie within the range estimated from the DM, nominally within ±30% of $d = 1.24$ kpc.

For a fixed flux, the highest effective temperature corresponds to the smallest stellar angular diameter, i.e., the smallest stellar radius at the greatest distance. The smallest secondary radius corresponds to $M_{\rm NS} = 1.4\,M_\odot$, $i = 90^\circ$, $M_c = 0.161\,M_\odot$, and the largest distance, ∼1.6 kpc; for these parameters, the observed flux is matched with $T_{\rm eff} = 4670$ K (assuming $A_R = 0.75$ mag). The largest angular diameter—with $M_{\rm NS} = 2.6\,M_\odot$, $i = 55^\circ$, $M_c = 0.297\,M_\odot$, and $d = 870$ pc—yields $T_{\rm eff} = 3560$ K. This range of temperatures corresponds to main-sequence spectral types between K2 and M2 (Pickles 1998); the secondary's spectrum most likely resembles a late K star.

However, at $d = 1.6$ kpc, the absolute $R$ magnitude of PSR J1628−3205 is +7.4, which, if it were an isolated main-sequence star, would correspond to type K7 with $M = 0.6\,M_\odot$ and $T_{\rm eff} = 4000$ K. At $d = 870$ pc, the absolute $R$ magnitude is +8.8, which corresponds to type M2 with $M = 0.4\,M_\odot$ and $T_{\rm eff} = 3550$ K. Main-sequence stars are more massive, and generally cooler than we have derived from modeling the light curve. The companion to PSR J1628−3205, having $M_c < 0.3\,M_\odot$, is less dense than a main-sequence star of its mass, and probably hotter.

If we allow a larger uncertainty in distance, say $620 < d < 2500$ pc, the effective temperature limits become 3270 K and 5340 K, which corresponds to main-sequence spectral types between M3 and G8. However, the conclusion remains that the companion star is less dense and hotter than a main-sequence star of the same mass.

A representative model corresponding to the nominal distance of 1.24 kpc is shown in Figure 3. It has $M_{\rm NS} = 1.4\,M_\odot$, $M_c = 0.167\,M_\odot$, $i = 75^\circ$, and $T_{\rm eff} = 4230$ K. Figure 2 shows the same model parameters fit to the previous year's data from the 1.3 m, except that $T_{\rm eff}$ is reduced by 100–4130 K in order to match the overall lower flux. The difficulties in fitting presented by the asymmetries described in Section 2.1 are most evident in Figure 3, but also to some extent in Figure 2. Since the ≈0.1 mag difference between the two minima is accounted for by ellipsoidal modulation, it is not possible to add heating from a point source without making the model exceed the observed flux in the phase interval 0.75–1.0, and especially the peak at $\phi = 1.0$. Neither ellipsoidal modulation nor axisymmetric pulsar heating can fit the unequal peaks at $\phi = 0.5$ and 1.

We do not have enough data to model the PSR J1301+0833 system in a similar manner. In particular, with only one filter, and with no detection of the companion near inferior conjunction, we do not have a handle on its base temperature and Roche-lobe-filling factor.

## 4. DISCUSSION

Among the optical light curves of redback MSPs, some are dominated by pulsar heating and some are not. In the former group are PSRs J1023+0038 (Thorstensen & Armstrong 2005), J2215+5135 (Breton et al. 2013; Schroeder & Halpern 2014), J2339−0533 (Romani & Shaw 2011; Kong et al. 2012; Ray et al. 2014), and XSS J12270−4859 (Bassa et al. 2014). Ones without a dominant heating effect are PSRs J1723−2837 (Crawford et al. 2013), J1816+4510 (Kaplan et al. 2012, 2013), and J2129−0428 (Bellm et al. 2013). This disparity can be understood in terms of the balance of a number of competing factors, including the intrinsic luminosity of the companion, the mass ratio and orbital separation, and the spin-down luminosity of the pulsar. We have seen some evidence that PSR J1628−3205 is an intermediate case, showing mainly ellipsoidal modulation, but possibly some heating.

Here we make a back-of-the-envelope calculation to evaluate whether we should expect pulsar heating to make an observable contribution to the optical luminosity of PSR J1628−3205. The representative model from Section 3 has a luminosity $L_{\rm bol} = 4\pi\, r_L^2\, \sigma\, T_{\rm eff}^4 = 1.5\times10^{32}$ erg s$^{-1}$, where $r_L = 2.6\times10^{10}$ cm, the radius of the Roche lobe according to Eggleton (1983). This value of luminosity is also obtained by direct summation over the surface of the model star. The contribution of pulsar irradiation $L_{\rm irr}$ to the optical luminosity can be expressed in terms of the heating efficiency $\eta$ of an assumed isotropic pulsar wind as $L_{\rm irr} = \eta\,\dot{E}\,r_L^2/4a^2$, where $a$ is the orbital separation, and $\dot{E} \leqslant 1.3\times10^{34}$ erg s$^{-1}$. This is an upper limit because of the unknown contribution of the kinematic period derivative, $\dot{P}_k = P\,v_\perp^2/d\,c$, where $P = 3.2$ ms. Assuming the tangential velocity $v_\perp \sim 100$ km s$^{-1}$ estimated in Section 2.1, $\dot{P}_k = 2.9\times10^{-21}$, which is 27% of the observed value, reducing $\dot{E}$ by the same percentage. For the representative model $r_L/a = 0.218$, $L_{\rm irr} = 1.1\times10^{32}\,\eta$ erg s$^{-1}$, and pulsar heating is comparable to the observed luminosity $L_{\rm bol}$ only if the efficiency of the process is of the order of unity, which is not likely for a number of reasons. First, the heating may be mediated by an intra-binary shock between the pulsar wind and the wind from the companion, which could radiate in all directions. Second, for stars with deep convective envelopes, as should be the case here (Chen et al. 2013), the effective efficiency of re-radiation is $\lesssim$0.5 (Ruciński 1969). Third, some of the energy absorbed goes into the ablated stellar wind. Due to uncertainties in the efficiencies of these processes, the true luminosity and beaming of the pulsar wind, and the distance, we cannot conclude whether heating should be observed in PSR J1628−3205.

Breton et al. (2013) estimated an efficiency in the range $0.1 \leqslant \eta \leqslant 0.3$ for the four systems they studied. For the nominal distance, the phenomena seen in the light curve of PSR

J1628−3205 that are *not* explained by ellipsoidal deformation could be effects of heating with $\eta$ in this range. The residual asymmetries may be caused indirectly by the material ablated from the companion. If a wind flows off the companion in a cometary tail that lags the orbital motion, then it is possible that the intra-binary shock is displaced toward the trailing side of the companion. A clear example of asymmetric heating can be seen in the orbital light curve of PSR J1023+0038, in which the maximum occurs before phase 0.75. Both in optical and in X-rays (Woudt et al. 2004; Bogdanov et al. 2011), the trailing side of the companion is brighter than the leading side.

Alternatively, a large starspot could produce an asymmetric temperature distribution. Since a starspot would also be associated with magnetic field intrinsic to the companion, it is also possible that such a magnetic field could channel the pulsar wind and cause enhanced local heating, as was speculated by Tang et al. (2014) to explain an apparent hot patch on the companion of PSR J1544+4937. For an intrinsic large-scale magnetic field to channel the pulsar wind, it must have a pressure at ∼1 stellar radius above the surface of the companion at least comparable to the pressure of the relativistic pulsar wind, i.e., $B^2/8\pi \geqslant \dot{E}/4\pi\,(a-2r_L)^2\,c$. For the representative model, this corresponds to $B \geqslant 12$ G, a not unreasonable value.

A similar calculation of the efficiency of pulsar heating can be made for the peak optical luminosity of PSR J1301+0833 at orbital phase 0.75. Assuming $i \approx 90^\circ$, and a DM distance of 0.67 kpc, we correct the observed $R = 21.8$ for $A_R \approx 0.1$. Converting to flux density using $f_{\lambda,\rm eff}^{\rm Vega} = 2.15 \times 10^{-9}$ erg cm$^{-2}$ s$^{-1}$ Å$^{-1}$ (Fukugita et al. 1995), the flux density at $\lambda_{\rm eff} = 6410$ Å is $f_\lambda = 4.5 \times 10^{-18}$ erg cm$^{-2}$ s$^{-1}$ Å$^{-1}$. If half of the star is illuminated by the pulsar wind and is re-radiating, its luminosity is $L_{\rm bol} = 1.1 \times 10^{30}$ erg s$^{-1}$ if $T_{\rm eff} = 5000$ K, or $L_{\rm bol} = 1.6 \times 10^{30}$ erg s$^{-1}$ if $T_{\rm eff} = 10{,}000$ K. For $M_{\rm NS} = 2\,M_\odot$, we have $M_c = 0.0305\,M_\odot$, and $r_L/a = 0.157$. If the companion fills its Roche lobe, then $L_{\rm irr} = 3.2 \times 10^{32}\,\eta$ erg s$^{-1}$. Black widow pulsars do not necessarily fill their Roche lobes, but there is room for this one to underfill by a large factor and still shine by reprocessed pulsar irradiation even if the efficiency for that process is ∼1%.

## 5. CONCLUSIONS AND FUTURE WORK

We have discovered the optical companions of two *Fermi* MSPs and confirmed the identifications based on their orbital photometric variability. Our *R*-band light curve of PSR J1301+0833 displays an amplitude of at least 2.4 mag, with a maximum at superior conjunction of the companion. PSR J1301+0833 appears to be a classic black widow system. Its companion is a faint, probably sub-stellar object around an MSP of high $\dot{E}$, which explains why its light is dominated by pulsar heating. The efficiency of this process is required to be only ∼1%. Deeper optical observations and multicolor light curves are needed before this system can be modeled, because we have not detected the unheated side of the secondary. So we do not know its effective temperature or Roche-lobe-filling factor.

The optical modulation of PSR J1628−3205 is very different. It is characterized by two peaks and two troughs per orbit, whose phase relationship to the pulsar ephemeris clearly establishes that ellipsoidal distortion is the cause of the variation. The amplitude of modulation is consistent with a near Roche-lobe-filling secondary star in a high-inclination orbit, which we conservatively estimate as $i > 55^\circ$. This limits the mass of the secondary to $0.16 < M_c < 0.30\,M_\odot$. It is less dense than a main-sequence star of the same mass.

It is not yet possible to derive system parameters more precisely for PSR J1628−3205 because its light curve also displays distortions that are not characteristic of ellipsoidal variations. An order-of-magnitude estimate for possible pulsar heating in this system justifies why this process does not make a major contribution to the radiation from the photosphere, because it would require an efficiency of order one. However, in addition, it is difficult to improve the fit to the light curve with even a small amount of isotropic heating from the pulsar. Instead off-center heating is required, or else an intrinsic, asymmetric surface-temperature distribution.

We used distance constraints from the pulsar DM to limit the effective temperature of the comparison star of PSR J1628−3205 to $3560 < T_{\rm eff} < 4670$ K. It should have the optical spectrum of a late K star. Multicolor photometry and spectra are needed to further investigate the cause of the distortions in the light curve and pin down the system parameters, including the mass of the NS. Evidence for an overall increase in brightness of ∼0.2 mag between 2013 and 2014 is present in our observations. This raises the possibility that we are seeing an increase in the photospheric temperature or Roche-lobe-filling factor that may eventually cause sufficient Roche-lobe overflow to form a partial accretion disk and shut off the radio pulsar mechanism, as has been observed recently in several similar redback systems.

This work is based on observations obtained at the MDM Observatory, operated by Dartmouth College, Columbia University, Ohio State University, Ohio University, and the University of Michigan. J.R.T. gratefully acknowledges support from NSF grant AST-1008217. We thank the referee for several helpful suggestions.

## REFERENCES

Alpar, M. A., Cheng, A. F., Ruderman, M. A., & Shaham, J. 1982, Natur, 300, 728
Archibald, A. M., Stairs, I. H., Ransom, S. M., et al. 2009, Sci, 324, 1411
Bassa, C. G., Patruno, A., Hessels, J. W. T., et al. 2014, MNRAS, 441, 1825
Bellm, E., Djorgovski, S. G., Drake, A., et al. 2013, BAAS, 221, 154.10
Benvenuto, O. G., De Vito, M. A., & Horvath, J. E. 2014, ApJL, 786, L7
Bogdanov, S., Archibald, A. M., Hessels, J. W. T., et al. 2011, ApJ, 742, 97
Bogdanov, S., Esposito, P., Crawford, F., et al. 2014a, ApJ, 781, 6
Bogdanov, S., Patruno, A., Archibald, A. M., et al. 2014b, ApJ, 789, 40
Breton, R. P., van Kerkwijk, M. H., Roberts, M. S. E., et al. 2013, ApJ, 769, 108
Casagrande, L., Flynn, C., & Bessell, M. 2008, MNRAS, 389, 585
Chen, H.-L., Chen, X., Tauris, T. M., & Han, Z. 2013, ApJ, 775, 27
Cordes, J. M., & Lazio, T. J. W. 2002, arXiv:astro-ph/0207156
Crawford, F., Lyne, A. G., Stairs, I. H., et al. 2013, ApJ, 776, 20
Deller, A. T., Archibald, A. M., Brisken, W. F., et al. 2012, ApJL, 756, L25
Eggleton, P. P. 1983, ApJ, 268, 368
Eichler, D., & Levinson, A. 1988, ApJL, 335, L67
Fukuguti, M., Shimasaku, K., & Ichikawa, T. 1995, PASP, 107, 945
Gentile, P. A., Roberts, M. S. E., McLaughlin, M. A., et al. 2014, ApJ, 783, 69
Geppert, U., & Urpin, V. 1994, MNRAS, 271, 490
Halpern, J. P., Gaidos, E., Sheffield, A., Price-Whelan, A. M., & Bogdanov, S. 2013, ATel, 5514, 1
He, C., Ng, C.-Y., & Kaspi, V. M. 2013, ApJ, 768, 64
Hessels, J. W. T., Roberts, M. S. E., McLaughlin, M. A., et al. 2011, in AIP Conf. Proc. 1357, Radio Pulsars: An Astrophysical Key to Unlock the Secrets of the Universe, ed. M. Burgay et al. (Melville, NY: AIP), 40
Kaplan, D. L., Bhalerao, V. B., van Kerkwijk, M. H., et al. 2013, ApJ, 765, 158
Kaplan, D. L., Stovall, K., Ransom, S. M., et al. 2012, ApJ, 753, 174
Kluzniak, W., Ruderman, M., Shaham, J., & Tavani, M. 1988, Natur, 334, 225
Kong, A. K. H., Huang, R. H. H., Cheng, K. S., et al. 2012, ApJL, 747, L3
Landolt, A. U. 1992, AJ, 104, 340
Lattimer, J. M., & Prakash, M. 2007, PhR, 442, 109

Linares, M. 2014, ApJ, in press (arXiv:1406.2384)
Monet, D. G., Levine, S. E., Canzian, B., et al. 2003, AJ, 125, 984
Papitto, A., Ferrigno, C., Bozzo, E., et al. 2013, Natur, 501, 517
Phinney, E. S., Evans, C. R., Blandford, R. D., & Kulkarni, S. R. 1988, Natur, 333, 832
Pickles, A. J. 1998, PASP, 110, 863
Podsiadlowski, Ph., Rappaport, S., & Pfahl, E. D. 2002, ApJ, 565, 1107
Predehl, P., & Schmitt, J. H. M. M. 1995, A&A, 293, 889
Radhakrishnan, V., & Srinivasan, G. 1982, CSci, 51, 1096
Ransom, S. M., Ray, P. S., Camilo, F., et al. 2011, ApJL, 727, L16
Ray, P. S., Abdo, A. A., Parent, D., et al. 2012, arXiv:1205.3089
Ray, P. S., Belfiore, A. M., Saz Parkinson, P., et al. 2014, BAAS, 223, 140.07
Roberts, M. S. E. 2011, in AIP Conf. Proc. 1357, Radio Pulsars: An Astrophysical Key to Unlock the Secrets of the Universe, ed. M. Burgay et al. (Melville, NY: AIP), 127
Roberts, M. S. E. 2013, in IAU Symp. 291, Neutron Stars and Pulsars: Challenges and Opportunities After 80 Years, ed. J. van Leeuwen (Cambridge: Cambridge Univ. Press), 127
Romani, R. W. 1990, Natur, 347, 741
Romani, R. W., Filippenko, A. V., Silverman, J. M., et al. 2012, ApJL, 760, L36
Romani, R. W., & Shaw, M. S. 2011, ApJL, 743, L26
Roy, J., Bhattacharyya, B., & Ray, P. S. 2014, ATel, 5890, 1
Ruciński, S. M. 1969, AcA, 19, 245
Schlafly, E. F., & Finkbeiner, D. F. 2011, ApJS, 737, 103
Schroeder, J., & Halpern, J. 2014, ApJ, 793, 78
Stappers, B. W., Archibald, A. M., Hessels, J. W. T., et al. 2013, ApJ, 790, 39
Tang, S., Kaplan, D. L., Phinney, S., et al. 2014, ApJL, 791, L5
Thorstensen, J. R., & Armstrong, E. 2005, AJ, 130, 759
Wang, Z., Archibald, A. M., Thorstensen, J. R., et al. 2009, ApJ, 703, 2017
Woudt, P. A., Warner, B., & Pretorius, M. L. 2004, MNRAS, 351, 1015